Research Article

Investigation of the kinetics and thermodynamics of the adsorption of ampicillin on Chitosan/Coconut Shell Ash composite (CCSAC)

A. Moshkriz✉,1

1. Department of Chemical Engineering, Faculty of Engineering, Arak University, Arak, Iran.

Chitosan/Coconut Shell ASH composite (CCSAC) has the potential to be a viable alternative adsorbent for removing Ampicillin (AMP) from aqueous solutions. In this study, CCSAC will be evaluated as a potential new adsorbent, and its adsorption mechanism for AMP will be investigated. The effects of AMP concentration, adsorption time, solution pH, and temperature on CCSAC adsorption are also investigated. The removal efficacy of AMP by CCSAC depends on the initial concentration of AMP in the solution. During the initial phase of the AMP adsorption process, the concentration of AMP decreases drastically within the first 150 minutes, then gradually decreases until equilibrium is reached after 600 minutes. In general, the adsorption capacity of CCSAC is dependent on the solution's pH, temperature, and ion concentration, particularly when the pH value is high. It was found that the absorption capacity doubled at a temperature of 45°C. Furthermore, it has been demonstrated that low-acid and high-alkaline solutions can accelerate the adsorption of AMP onto CCSAC. As the highest adsorption capacity recorded in this study is 16.8 mg/g, it is significantly higher than other adsorbates reported in the literature, indicating the feasibility of CCSAC as a new type of adsorbent. The Langmuir isotherm model provides the most plausible explanation for how adsorption takes place. Pseudo-second-order models fit nicely with the experimental data, suggesting a primarily physical and chemical control over the adsorption process is occurring. As a result, such findings can serve as a useful guide for extending the applicability of CCSAC to a broader range of areas.

Keywords: Hydrogel, Coconut Shell ASH, Chitosan, Ampicillin, adsorption, Composites

Introduction

As a broad-spectrum antibiotic, ampicillin (AMPs) features a wide range of therapeutic effects, and they are widely used in human and veterinary medicine to control disease, as well as in livestock feed, due to their perceived therapeutic effects [1]. Although AMPs are stable in the digestive tract, they are poorly absorbed by the body due to their stability. Only a small amount of AMPs ingested are metabolized or absorbed by the body. More than 50% of the AMPs that are ingested are excreted through the feces and urine as raw materials [2]. There is evidence that AMPs have been detected in soil, sediments, surface waters, and drinking water after they have been discharged into the environment [3]. Several studies suggest that AMPs may pose a significant risk to ecosystems as well as human health [4], even at very low or permissible concentrations. AMPs have been shown to cause allergic reactions in humans [5], as well as the development of antibiotic-resistance genes in bacteria [6], which the World Health Organization considers to be one of the greatest threats to human health in the 21st century.

It is important to note that AMPs have a low degradation rate and are lethal to most microorganisms due to their antibacterial nature, which makes it difficult for them to be effectively removed during activated sludge treatment [7]. Generally, AMPs are difficult to remove from water in traditional wastewater treatment plants (WWTPs), which have become the dominant source of residual AMPs. Various physical and chemical treat-

Received: 02.03.2023

Accepted: 05.01..2023

DOI: 10.29252/yujs.1.11.

E-mail: alimoshkriz1994@gmail.com

ment methods have been used to enhance the removal efficiency of AMPs in WWTPs, including photocatalytic oxidation [8], ozonation, and adsorption [9]. In addition to activated carbon [10], bamboo charcoal, clays, polymers, aluminum oxide [11], nanomaterials and microparticles, and even resins [12], adsorption of AMPs by porous materials have been proven to be one of the most efficient methods of AMP removal [11]. It should be noted, however, that these adsorbents can be excessively expensive in practice, particularly if they are used on a macroscale for water treatment. The development of more cost-effective and efficient AMP adsorbents is therefore necessary. As an agricultural waste, coconut shell ash (CCSAC) could be a candidate for use as an adsorbent [13]. Approximately one-fifth of the world's gross coconut production of 545 million tons is consumed as fuel in boiler furnaces [14]. In addition to removing organic pollutants from aqueous systems, coconut shell is an effective adsorbent for removing inorganic pollutants, including phenol [15], dye, nitrate, and toxic metals [15]. It has been demonstrated that crop residue-derived ashes can adsorbate AMPs and sulfamethoxazole in soil [16], suggesting that CCSAC could be a potentially effective adsorbent for removing AMPs from aqueous systems. The purpose of this study is to determine. This study represents the initial exploration of AMP adsorption characteristics on CCSAC, as well as the potential application of CCSAC for AMP removal in aqueous environments. We specifically investigate the impact of factors such as initial AMP concentration, adsorption time, solution temperature, and pH on the efficiency of AMP adsorption. The outcomes of this investigation will enhance our comprehension of the physicochemical adsorption mechanisms associated with the novel CCSAC adsorbent.

Materials and Methods

Ampicillin (AMP) hydrochloride of analytical grade was obtained from Aladdin-reagent Co., Ltd. (China), and CCSAC was obtained from Jiangsu Shengli Materials Co., Ltd. (China). To prepare for the tests, a stock solution containing 50 mg/L of AMP was prepared with deionized water first. A temperature-controlled orbital shaker (ZD-85A, Jintan Ronghua Instrument Manufacture Co., Ltd.) was used to conduct the adsorption experiments in 50 mL polypropylene centrifuge tubes soaked in HNO3 solution. During the storage and adsorption processes, these centrifuge tubes were wrapped with aluminum foil to prevent light-induced decomposition (Scheme 1).

The results of the adsorption experiments were replicated three times, with the mean values representing the final results.

CCSAC was used in Bach experiments at a concentration of 3 g/L (0.06 g of CCSAC was added to 20 mL of AMP solution), and AMP concentrations ranged from 50 to 150 mg/L. A predetermined time was set for the taking of samples, and after the adsorption experiments were completed, all suspensions were filtered through a membrane of 0.45 microns. To determine the pH effect of AMP, the initial concentration of the drug was 100 mg/L, and the pH values of the solvent were calibrated with NaOH and HCl aqueous solutions to achieve pH values of 2 - 12. An experiment was conducted for ten hours at three different temperatures (25, 35, and 45°C) to investigate the impact of adsorption temperature. A pH adjustment of 2.0 was performed on samples before detection by adding concentrated HCl to improve the analytical results of AMPs that were stable in HCl. A UV-vis spectrophotometer (UV-2550, Shimadzu, Japan) was used to detect the samples. The maximum absorption wavelength of AMP was determined by performing a full-band ultraviolet scan of the sample. The calibration plot displays a linear relationship between absorbance and AMP concentration over the range 0–150 mg/L. The adsorption capacity of CCSAC (Qt, mg/g) and its removal rate of AMP (r, %) were counted using Eqs. (1) and (2), respectively [17].

$$Q_t = \frac{(C_0 - C_t) \times V}{m} \quad (1)$$

$$r = \frac{(C_0 - C_t)}{C_0} \times 100\% \quad (2)$$

The initial concentration and residual concentration of AMP solution (mg/L) at a given time are denoted by C0 and Ct, respectively; V represents the volume of AMP solution (20 mL), and m represents the mass of CCSAC (g). Desorption studies of AMP from CCSAC

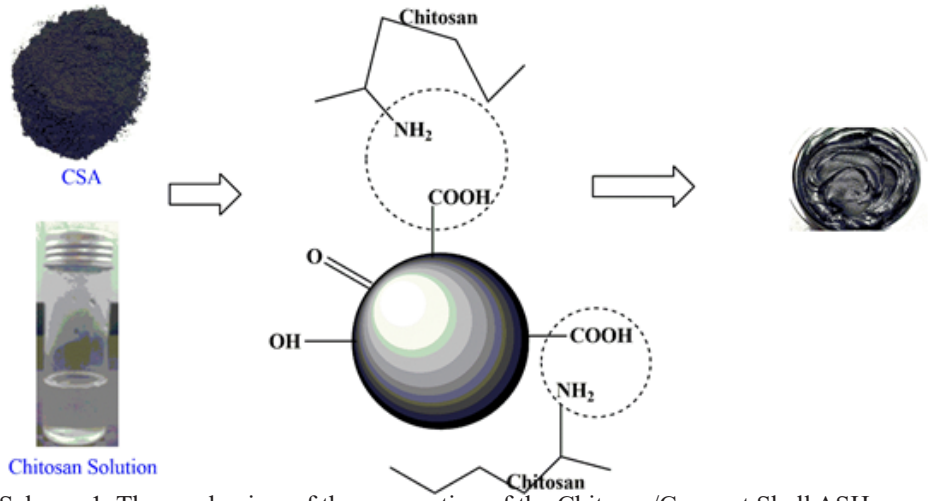

Scheme.1. The mechanism of the preparation of the Chitosan/Coconut Shell ASH composite.

The initial concentration and residual concentration of AMP solution (mg/L) at a given time are denoted by C0 and Ct, respectively; V represents the volume of AMP solution (20 mL), and m represents the mass of CCSAC (g). Desorption studies of AMP from CCSAC were performed by immersing dried hydrogel pieces containing adsorbed AMP in 100 mL of 0.1 mol L−1 NaOH solution, ethanol, methanol, and isopropanol solutions at specific intervals of time. Moreover, desorption assays of AMP from CCSAC were performed by applying filtration. To study the structure of CCSAC, an X-ray diffractogram (XRD) was obtained using an X-ray diffractometer (D/max 2500VL/PC, Rigaku, Japan) and CuKα as the radiation source. The scanning scope was $5° \leq 2\theta \leq 85°$ at room temperature. A distinct peak characterizes CCSAC XRD patterns (Figure 1) at around 22°, corresponding to crystalline silica. As can be seen from the Figure, the peak at 2θ=20˚ shifted to the lower 2θ (about 10˚), concluding that polymer chains make crystal plates of coconut Sell Ash distant.

Results and Discussions

Effects of initial AMP concentration and adsorption time

According to Figure 2, the effects of initial AMP concentration and adsorption time on the adsorption of AMP onto CCSAC ranged from 0 to 900 min. There is no doubt that the AMP concentration of the solution decreases rapidly in the first 60 minutes, followed by a gradual decrease over the following 60 minutes.

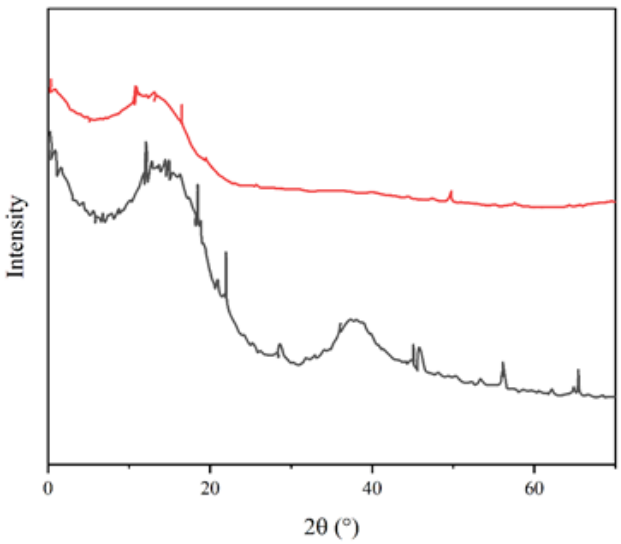

Figure. 1. X-ray diffraction pattern of Coconut Sell Ash and CCSAC hydrogel.

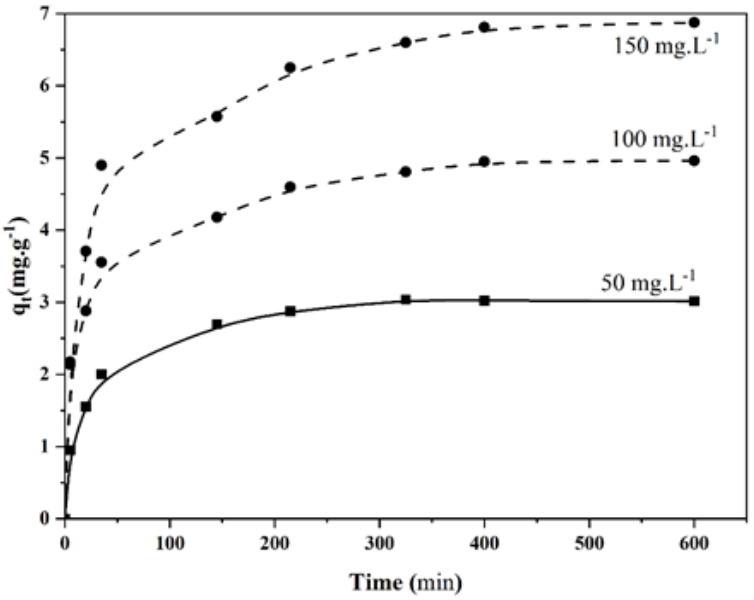

Figure. 2. Emulation of qt against time for CCSAC hydrogel at different initial concentrations of AMP

There is no doubt that the AMP concentration of the solution decreases rapidly in the first 60 minutes, followed by a gradual decrease over the following 60 minutes. Over 600 minutes of adsorption, the AMP concentration does not change significantly, indicating equilibrium adsorption for CCSAC. In other words, the amount of AMP adsorption on the adsorbent must equal the amount of AMP adsorption on the adsorbent must equal the amount of AMP adsorption on the adsorbent. As a result, 600 minutes were selected as the adsorption equilibrium time in all subsequent experiments. In addition, the time required to achieve equilibrium hardly varies with the initial concentration of the AMP solution. CCSAC's surface has a large amount of vacant area for adsorption, which may have contributed to the rapid initial decrease in AMP solution concentration.

In contrast, the reduced available surface area may have contributed to the delayed decrease in AMP solution concentration. Furthermore, it has been suggested that the decreased adsorption is caused by repulsive forces between the molecules of AMP in the solution and those adsorbed on the surface of CCSAC [18]. It has been suggested that the aggregation of AMP molecules around CCSAC particles can impede the diffusion of AMP molecules into the adsorbent structure. The removal efficiency of AMP solution (r) decreases from 63.4% to 38.7% as the concentration increases from 50 to 150 mg/L, whereas the adsorption capacity of CCSAC (Qe) increases from 3.2 to 7.1 mg/g (Table 1). AMP molecules pass more readily from the aqueous solution to the CCSAC particle surface when there is a high concentration of AMP solution [19], leading to higher AMP absorption. Despite this, the removal efficiency (r) decreases with an increase in the initial concentration of AMP. The surface of CCSAC has many vacant sites at low AMP concentrations, and these vacant sites are saturated at higher AMP concentrations, resulting in a decrease in removal efficiency [20].

Ionic strength and pH effects

Adsorption processes can be affected by the pH of a solution since the pH of a solution may affect the surface charge of an adsorbent and the species of adsorbate [21]. A study has demonstrated that the pH of a solution is the most influential factor in adsorption [22]. By varying the initial solution pH from 2 to 12, the effects of pH on AMP adsorption onto CCSAC were evaluated (Figure 3).

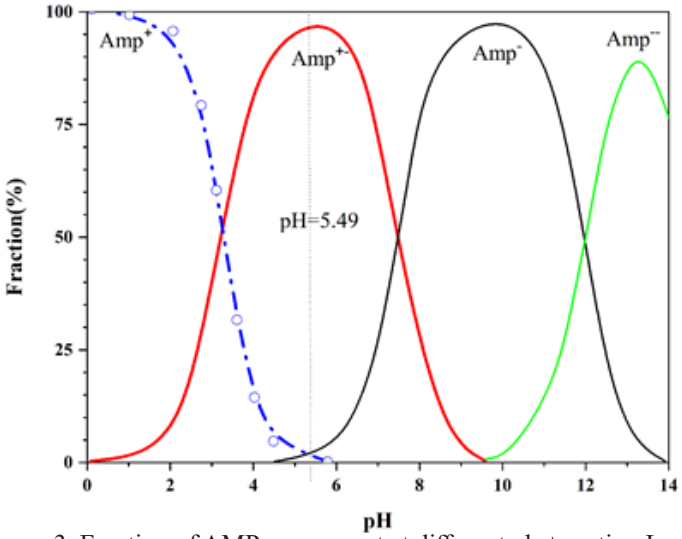

Figure 3. Fraction of AMP component at different ph.+: cation Ion, -: Anion Ion and +-: Inert Ion.

As shown in Figure. AMP species at different pH values are shown in Figure 4a. The AMP molecule is cationic (AMPH3 +) when pH b 3.3. Between pH 3.3 and 7.7, the AMP molecule is mainly found as an anion, AMPH', and AMP2'. By increasing the pH of the solution, AMP adsorption increases. Due to electrostatic repulsion between cationic AMP species and positive surface charges on CCSAC, an acidic pH does not favor the adsorption of AMP molecules to the surface. A decrease in cationic AMP species is observed as pH rises.

Furthermore, AMP molecules exist in solution as a zwitterion, and AMP ions exchange only with CCSACs with a positive surface charge. AMP molecules exist primarily in the anion form on CCSAC surfaces in high pH conditions. After corrosion by strong alkalis and higher pH, the surface of CCSAC is dotted with tiny holes that can enhance CCSAC's physical and chemical adsorption significantly, such as surface complexation on the edge sites.

Moreover, the adsorption of AMP decreases with increasing ionic strength, particularly at low pH values. Under alkaline conditions, this effect is more pronounced. Accordingly, Zhao et al. have reported in the literature that Na+ ions compete with AMP molecules for CCSAC adsorption sites [23].

Temperature-related effects

There were three temperatures used in the adsorption experiments, 25, 35, and 45 ℃, with a specified equilibrium time of 10 hours. Based on the results shown in Table 2, the maximum adsorption occurs at a temperature of 45 ℃, and the maximum removal rate is 89.2%, 85.6%, and 61.37%, respectively, corresponding to 50, 100, and 150 mg/L concentrations of AMP solution. There appears to be an increase in the rate of uptake of AMP with increasing temperature. This may be attributed to the strengthening of the adhesive forces between the CCSAC active sites and AMP species, as well as those between adjoining AMP molecules. By increasing the temperature, AMP molecules diffuse faster, and the retarding forces acting on them are reduced, thereby providing more activated adsorption sites on the adsorbent.

Models of adsorption isotherms

According to an adsorption isotherm, the amount of adsorbate adsorbed onto the adsorbent depends on the concentration of adsorbate in the solution. At three different temperatures (25, 35, and 45℃), 0.04 g of the CCSAC was added to 20 mL of AMP solutions with a concentration ranging from 50 to 150 mg/L. An adsorption isotherm model is used to analyze the equilibrium data of AMP, and a feasibility assessment is provided in Figure 4.

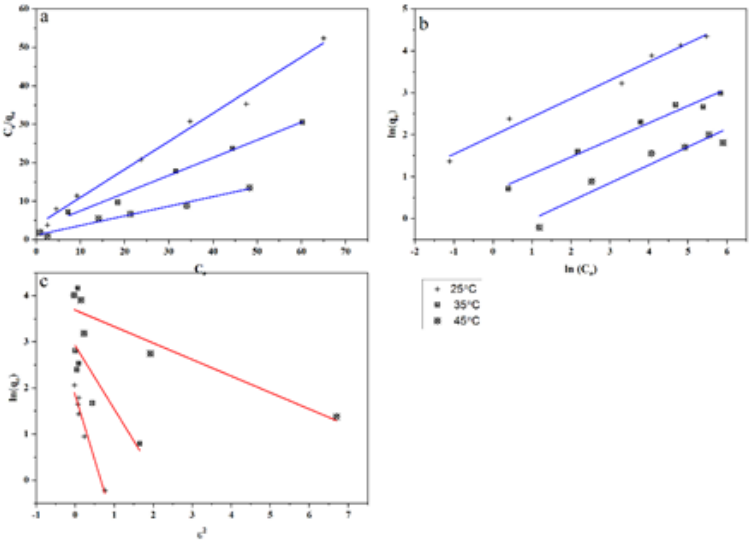

Figure 4. The plot of different isotherm models for AMP adsorption at three temperatures: (a) Langmuir; (b) Freundlich; (c) D-R (CCSAC dosage = 3 g/L, initial pH = 5.0 and equilibration time = 600 min).

The Langmuir isotherm model for adsorption

Generally, the Langmuir adsorption isotherm model is applied to monolayer adsorption over an adsorbent surface containing a finite number of identical sites and no further interactions between the adsorbed molecules. According to this hypothesis, all of the binding sites at the surface of an adsorbent are homogeneous in terms of activation energy, and there is no transmigration of adsorbate into the surface plane upon adsorption [24]. Considering these assumptions, the model is represented as Eq. 3 based on these assumptions.

$$\frac{C_e}{Q_e} = \frac{1}{Q_m \times K_L} + C_e/Q_m \qquad (3)$$

In this equation, Ce (mg/L) is the concentration of AMP in the equilibrium solution, whereas Qe (mg/g) is the amount of AMP adsorbed per unit mass of CCSAC. The adsorption constants KL (L/mg) and Qm (mg/g) are used to characterize the surface strength and the maximum adsorption capacity of the surface. A plot of Ce/Qe versus Ce is used to determine KL and Qm. As a consequence, Weber and Chakraborti [24] have defined the essential characteristic of the Langmuir isotherm as the equilibrium parameter RL, which is a dimensionless constant defined as Eq. (4):

$$R_L = \frac{1}{1+K_L C_0} \qquad (4)$$

The Langmuir constant, KL, and initial AMP concentration, C0, determine the shape of the isotherm, and the RL parameter indicates if adsorption is unfavorable (RL > 1), linear (RL = 1), favorable (0 < RL < 1), or irreversible (RL = 0). The RL values for this study were 0.420 and 0.067 for initial AMP concentrations of 50 mg/L and 150 mg/L, respectively, indicating favorable equilibrium sorption. The Langmuir model showed a monolayer adsorption capacity of 5.2-16.8 mg/g of AMP on CCSAC, and the high R2 value (>0.9) confirmed the Langmuir isotherm model›s applicability. Compared to other absorbents used for contaminant removal, CCSAC had the third-best performance and was inexpensive and abundantly available. Therefore, CCSAC could be a viable alternative for AMP removal.

Freundlich adsorption isotherm model

Unlike the Langmuir model, the Freundlich adsorption isotherm model is an empirical model used to describe the adsorption characteristics on a heterogeneous surface.

This model is represented by an equation with KF (mg/g) as the Freundlich sorption coefficient that indicates CCSAC›s adsorption capacity and n representing adsorption strength in the adsorption process. The value of n ranges from 1 to 10, indicating the favorability of the adsorption process. A smaller value of 1/n suggests higher expected heterogeneity. When n = 1, the expression is reduced to a linear adsorption isotherm. The values of n in Table 3 show a favorable adsorption process of AMP onto CCSAC at all three temperatures. The R2 values are consistently smaller than those of the Langmuir adsorption isotherm model. However, the experimental data fit more closely to the Langmuir model than the Freundlich model, indicating that AMP uptake preferably follows the monolayer adsorption process.

Table 1. Characteristic parameters of adsorption isotherm models (CCSAC dosage=2 g/L, initial pH =5.0, and equilibration time=10 h).

T(K)	Langmuir			Freundich			D-R		
	Qm (mg/g)	KL (L/mg)	R2	KF	1/n	R2	Qm (mg/g)	E (kj/mol)	R2
283	2.807	0.216	0.953	0.698	0.379	0.830	2.406	0.489	0.920
298	4.241	0.276	0.998	1.266	0.334	0.926	3.522	0.779	0.873
313	8.370	0.296	0.971	2.491	0.346	0.897	6.47	1.376	0.849

Dubinin–Radushkevich adsorption isotherm model

The Dubinin-Radushkevich adsorption isotherm model (Eq. 6) determines the adsorption mechanism by calculating the Gaussian energy distribution onto a heterogeneous surface. This model is suitable for high solute activities and an intermedi ate range of concentration levels.

$$lnQ_e = lnQ_m - K_{DR}^2 \qquad (6)$$

$$=\underline{\text{RTln}}\,(1+\frac{1}{C_e}) \qquad (7)$$

The constants Qm and KDR are obtained from the slope and intercept of the straight line by fitting lnQe and ε2 using a least-squares program. The linear plot of the D-R model shows that the mean free energy E increases with temperature, indicating that physical forces like Van der Waals and hydrogen bonds dominate the adsorption process.

$$E=\frac{1}{\sqrt{2K_{DR}}} \qquad (8)$$

The energy of adsorption, E, is usually used to distinguish physical adsorption from chemical adsorption.

Analysis of adsorption thermodynamics

The behavior of adsorption in relation to temperature can be analyzed using thermodynamic analysis. This was done for AMP-CCSAC adsorption at three different temperatures, calculating thermodynamic parameters such as changes in free energy, enthalpy, and entropy. The standard free energy change of adsorption (ΔG0), standard enthalpy change (ΔH0), and standard entropy change (ΔS0) were calculated using Equations (9) and (10), where R is the universal gas constant, T is temperature in Kelvin, and ΔG0, ΔH0, and ΔS0 are expressed in kJ/mol and J/(mol K), respectively.

$$\Delta G^\circ = -RTlnK \qquad (9)$$

$$\Delta G^\circ = \Delta H^\circ - T\Delta S^\circ \qquad (10)$$

The nature of adsorption can be identified by the value of ΔH0, where a range of 2.1-20.9 kJ/mol indicates physisorption. The thermodynamic equilibrium constant (K) was determined by plotting lnQe/Ce against Qe and extrapolating the relationship to Qe = 0. The values of ΔH0 and ΔS0 were then calculated from the linear plot of ΔG0 versus T. The results of the thermodynamic analysis showed that the adsorption process was favorable and spontaneous at all three temperatures, with a more favorable adsorption process at higher temperatures. This was supported by the finding that the adsorption capacity of AMP on CCSAC

increased with increasing temperature. A positive ΔS0 value indicates increased randomness at the adsorbent-adsorbate interface during the adsorption process, with the ΔS0 value of 40.098 J/ (mol K) in Table 5, indicating that the CCSAC-AMP adsorption process was extremely random in this study.

Adsorption kinetics

Numerous kinetic models have been employed to study adsorption processes and predict their behavior over time, as most solid phase transformations are time-dependent. This study employed pseudo-first order, pseudo-second order, and Weber Morris models

Table 2. Thermodynamic parameters of AMP adsorption on CCSAC at different temperatures.

Temperature (K)	K	ΔG° (Kj/mol)	ΔH° (Kj/mol)	ΔS° (J/mol k)
283	6.527	-4.414	6.907	40.098
298	7.822	-5.096		
313	8.658	-5.617		

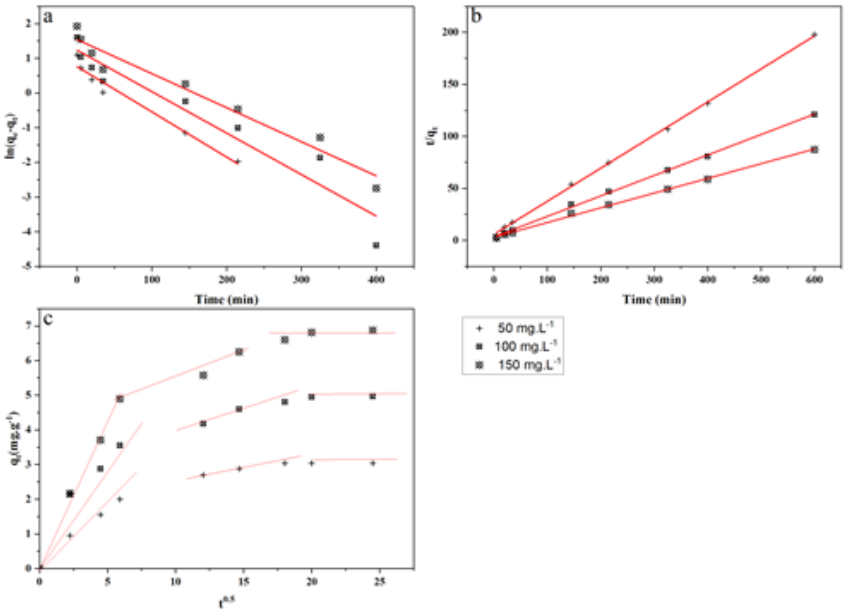

Figure 5. The plot of kinetic models of AMP adsorption onto CCSAC: (a) pseudo-first-order; (b) pseudo-second-order; (c) interparticle diffusion model (CCSAC dosage = 3 g/L, initial pH = 5.0 and temperature = 25°C)

to investigate the adsorption kinetics and understand the connection between the adsorbate and adsorbent. The pseudo-first and pseudo-second-order models are commonly used to represent the adsorption of adsorbate from an aqueous solution. The rate constant of pseudo-first-order adsorption, K1, and the pseudo-second-order rate constant, K2, were used to examine the adsorption capacity of CCSAC at equilibrium and over time, respectively. The R2 value for the pseudo-first-order model ranged from 0.85 to 0.98, indicating a strong correlation between the variables. In contrast, the pseudo-second-order model fit the adsorption process well with an R2 value of 0.99-1.00. The adsorption capacity increased with initial concentration, but the experimental data did not conform well to the pseudo-first-order model. The intra-particle diffusion rate

constant, Ki, was determined using the Weber-Morris model to evaluate whether intra-particle diffusion was the limiting factor in the adsorption process. A straight line through the origin indicated that only intra-particle diffusion-controlled adsorption. However, if the distribution requires multiple linear segments, two or more steps might be involved in the adsorption process. Therefore, the adsorption process was controlled by three stages, and intra-particle mass transfer resistance did not limit the adsorption rate.

Figure 6 shows the adsorption (A) and desorption (D) percentages of 2,4-D from chitosan-based hydrogel (CBH) and chitosan/magnetite-based composite hydrogel (CMCH).

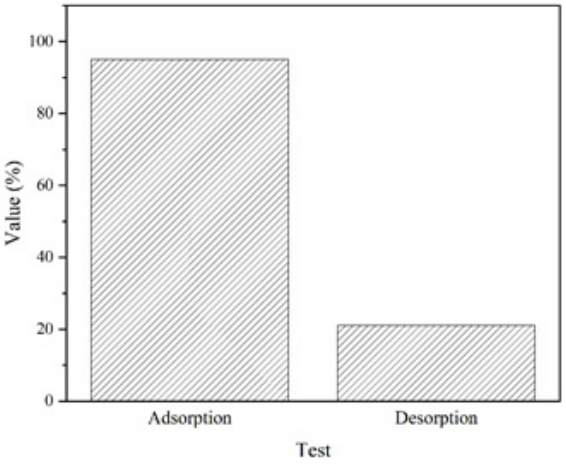

Figure 6. Adsorption and desorption percentages of AMP from CCSAC. Experimental adsorption conditions: 100 mg L−1 initial AMP concentration, pH = 5.0, 3g/L hydrogel mass, and temperature of 25°C. Experimental desorption conditions: pH = 9.7 and temperature of 25°C

Observations revealed physical adsorption of AMP onto the hydrogel, suggesting that desorption processes could vary in efficiency depending on the aqueous medium used. In general, desorption of AMP in alcoholic solutions exhibited insignificant percentages, indicating a weaker interaction between the solvent and AMP than between the hydrogel and AMP. To investigate AMP desorption further, experiments were conducted using a 0.2 mol L−1 NaOH solution, considering the herbicide pKa of 3.2. The desorption percentages of AMP from CCSAC in the alkaline solution were 8.5% and 21.7%, respectively. This suggests that the intermolecular interactions between the hydrogel and the pollutant are stronger than between the solvent and the pollutant.

Table 3 compares the properties of the current hydrogels used in the AMP adsorption process with those of existing products. These properties include the maximum capacity, the governing adsorption isotherm, and kinetic models. Table 3 compares different adsorbents for AMP removal from wastewater.

Conclusions

This study investigated the adsorption capacity of CCSAC as an inexpensive and natural adsorbate for the removal of AMP from an aqueous solution. The removal efficiency of AMP decreases from 156.5% to 93.4%, and the adsorption capacity of CCSAC increases from 4.42 to 9.36 mg/g when the initial concentration of AMP solution increases from 50 mg/L to 150 mg/L.

The acidic pH has not favored the adsorption of AMP because of electrostatic repulsion between cationic

Table 3. compaison

Adsorbant	Adsorption capacity (mg/g)	Isotherm model	Kinetic model	reference
Alg/Fe3O4@C@TD beads	Not reported	Not reported	Not reported	[35]
Fe3O4/SiO2/CTAB–SiO2	362.7	Langmuir	Not reported	[71]
Activated carbon from olive stone	57	Langmuir	Pseudo-first order	[72]
Nano MnO2 in carbon microspheres	16.09	Langmuir	Pseudo-first order	[73]
Vinewood carbon nanoparticles	8.41	Langmuir	Pseudo-second order	[33]

AMP species and positive surface charges on CCSAC. The removal rate of 50 mg/L AMP solution increases from 50.1% to 108.56% as the temperature rises from 25 to 45ºC. The maximum adsorption capacity of CCSAC is 11.2 mg/g at 45ºC, which is higher than most other adsorbates reported in the literature. Moreover, the Langmuir isotherm model fits the experimental data well. The adsorption process follows the pseudo-second-order model, indicating it is mostly controlled by physical and chemical interactions. Therefore, CCSAC can be used as a cheap adsorbent to remove AMP from aqueous solutions.

References

1. Mahmood A, Patel D, Hickson B, DesRochers J, Hu X. Recent progress in biopolymer-based hydrogel materials for biomedical applications. International Journal of Molecular Sciences. 2022;23(3):1415.

2. Samani FN, Darvishi R, Moshkriz A, Darvish M. Oxidized Pectin-Cross-Linked O-Carboxymethyl Chitosan/EDTriAA Intercalated LDH: An Antibiotic Adsorbent Hydrogel. Journal of Polymers and the Environment. 2023:1-18.

3. Darvishi R, Moghadas H, Moshkriz A. Oxidized gum arabic cross-linked pectin/O-carboxymethyl chitosan: An antibiotic adsorbent hydrogel. Korean Journal of Chemical Engineering. 2022;39(5):1350-60.

4. Ge H, Ding K, Guo F, Wu X, Zhai N, Wang W. Green and Superior Adsorbents Derived from Natural Plant Gums for Removal of Contaminants: A Review. Materials. 2022;16(1):179.

5. Alpaslan D, Olak T, Turan A, Ersen Dudu T, Aktas N. Use of coconut oil-based organo-hydrogels in pharmaceutical applications. Journal of Polymers and the Environment. 2021:1-15.

6. Krathumkhet N, Imae T, Paradee N. Electrically controlled transdermal ibuprofen delivery consisting of pectin-bacterial cellulose/polypyrrole hydrogel composites. Cellulose. 2021;28:11451-63.

7. Ramli RA, Lian YM, Nor NM, Azman NIZ. Synthesis, characterization, and morphology study of coco peat-grafted-poly (acrylic acid)/NPK slow release fertilizer hydrogel. Journal of Polymer Research. 2019;26:1-7.

8. Azizi N, Nasseri S, Nodehi RN, Jaafarzadeh N, Pirsaheb M. Evaluation of conventional wastewater treatment plants efficiency to remove microplastics in terms of abundance, size, shape, and type: A systematic review and Meta-analysis. Marine pollution bulletin. 2022;177:113462.

9. Thakali O, Brooks JP, Shahin S, Sherchan SP, Haramoto E. Removal of antibiotic resistance genes at two conventional wastewater treatment plants of Louisiana, USA. Water. 2020;12(6):1729.

10. Umerah CO, Kodali D, Head S, Jeelani S, Rangari VK. Synthesis of carbon from waste coconutshell and their application as filler in bioplast polymer filaments for 3D printing. Composites Part B: Engineering. 2020;202:108428.

11. Ly KL, Colon-Ascanio M, Ou J, Wang H, Lee SW, Wang Y, et al. Dissolvable alginate hydrogel-based biofilm microreactors for antibiotic susceptibility assays. Biofilm. 2023;5:100103.

12. Seydibeyoğlu MÖ, Dogru A, Wang J, Rencheck M, Han Y, Wang L, et al. Review on Hybrid Reinforced Polymer Matrix Composites with Nanocellulose, Nanomaterials, and Other Fibers. Polymers. 2023;15(4):984.

13. Saghian M, Dehghanpour S, Sharbatdaran M. Unique and efficient adsorbents for highly selective and reverse adsorption and separation of dyes via the introduction of SO 3 H functional groups into a metal–organic framework. RSC advances. 2020;10(16):9369-77.

14. Yang X, Dong Z, Zhang M, Du J, Zhao L. Selective recovery of Ag (I) using a cellulose-based adsorbent in high saline solution. Journal of Chemical & Engineering Data. 2020;65(4):1919-26.

15. Desmiarti R, Martynis M, Trianda Y, Li F, Viqri A, Yamada T. Phenol adsorption in water by granular activated carbon from coconut shell. Chemical Engineering. 2019;10(8):1488-97.

16. Nartey OD, Zhao B. Biochar preparation, characterization, and adsorptive capacity and its effect on bioavailability of contaminants: an overview. Advances in Materials Science and Engineering. 2014;2014.

17. Adlak K, Chandra R, Vijay VK, Pant KK. Suitability analysis of sustainable nanoporous adsorbents

for higher biomethane adsorption and storage applications. International Journal of Energy Research. 2022;46(11):14779-93.
18. Banin A, Lawless J, Mazzurco J, Church F, Margulies L, Orenberg J. pH profile of the adsorption of nucleotides onto montmorillonite: II. Adsorption and desorption of 5′-AMP in iron-calcium montmorillonite systems. Origins of Life and Evolution of the Biosphere. 1985;15:89-101.
19. Rahardjo AK, Susanto MJJ, Kurniawan A, Indraswati N, Ismadji S. Modified Ponorogo bentonite for the removal of ampicillin from wastewater. Journal of Hazardous Materials. 2011;190(1-3):1001-8.
20. Zhang Y, Kong X. Correlations of the dispersing capability of NSF and PCE types of superplasticizer and their impacts on cement hydration with the adsorption in fresh cement pastes. Cement and concrete research. 2015;69:1-9.
21. Wang Y-J, Jia D-A, Sun R-J, Zhu H-W, Zhou D-M. Adsorption and cosorption of tetracycline and copper (II) on montmorillonite as affected by solution pH. Environmental Science & Technology. 2008;42(9):3254-9.
22. Xue Y, Wu S, Zhou M. Adsorption characterization of Cu (II) from aqueous solution onto basic oxygen furnace slag. Chemical engineering journal. 2013;231:355-64.
23. Shang Y, Hasan MK, Ahammed GJ, Li M, Yin H, Zhou J. Applications of nanotechnology in plant growth and crop protection: a review. Molecules. 2019;24(14):2558.
24. Chen Y, Wang F, Duan L, Yang H, Gao J. Tetracycline adsorption onto rice husk ash, an agricultural waste: Its kinetic and thermodynamic studies. Journal of Molecular Liquids. 2016;222:487-94.